

Photocatalytic ethanol to H₂ and 1,1-diethoxyethane by Co(II) diphenylphosphinate/TiO₂ composite

Aihong Li ^{a,b}, Dongyang Li ^b, Jianwei Mao ^b, Zhimeng Ge ^b, Jianping Guo ^{b,c,*}, Bo Liu ^{a,*}

^a Department of Chemistry, School of Science, Beijing Jiaotong University, Beijing 100044, China

^b State Key Laboratory of Solid Waste Reuse for Building Materials, Beijing Building Materials Academy of Science Research, Beijing 100041, China

^c Institute of Applied Chemistry, Shanxi University, Taiyuan 030006, China



ARTICLE INFO

Article history:

Received 14 December 2020

Accepted 25 February 2021

Available online 5 March 2021

Keywords:

Solvothermal method

Cobalt(II) diphenylphosphinate/TiO₂ composite

Hydrogen production

1,1-Diethoxyethane

Photocatalysis

ABSTRACT

Through a facile solvothermal method, the novel composites of cobalt(II) diphenylphosphinate/TiO₂ have been synthesized and used for photocatalytic hydrogen production in ethanol solution. The chemical composition and surface morphology were analyzed by XPS, XRD, ICP-OES, EA, IR and SEM. The composite CoTi10 showed high photocatalytic activity in H₂ evolution that the quantity is ca. 1155.86 μmol/g for 3 h in ethanol solution under the illumination of UV-visible light source, which is 12 times higher than the commercial P25. The composites also exhibited unique selectivity for converting ethanol to 1,1-diethoxyethane in the photocatalytic process. Moreover, their good stabilities were revealed in the recycling test. It is thus clear that the composite can effectively inhibit the recombination of electron-hole pairs in photocatalytic reactions and lead to the enhanced hydrogen production rate.

© 2021 Elsevier Ltd. All rights reserved.

1. Introduction

Nowadays, due to the extensive application of non-renewable resources such as fossil fuels, environmental pollution and energy crisis are two major problems facing humanity. Finding effective ways to solve the problem of energy shortage has become an important research topic. Hydrogen energy is considered as a clean, renewable and environmentally friendly energy vector and energy carrier [1–3]. Among all the methods of hydrogen production, the photocatalytic H₂ generation is one of the effective ways to solve two major issues.

Since Fujishima and Honda discovered that TiO₂ can decompose water under ultraviolet light in 1972 [4], it has attracted extensive attention and considered one of the best potential semiconductor photocatalysts for hydrogen production. Because of its unique chemical stability [5], availability, high reactivity [6], low cost [7], non-toxic and harmless safety, TiO₂ has been widely used in p-type transparent conductor [8], lithium-ion micro-batteries [9], self-cleaning and anti-fouling [10]. However, the photocatalytic activity of TiO₂ is constrained to a certain level due to the rapid recombination of photogenerated electron-hole pairs and the wide energy band gap. To increase the photocatalytic activity, a great

number of studies have been proceeded on improving the photocatalytic hydrogen production performance of TiO₂. For example, the modified TiO₂ crystals by ethanol-quenching exhibited a very high visible-light-assisted H₂ generation rate of 180.5 μmol/g/h in water splitting, which is 50 times higher than that of pristine P25 (3.5 μmol/g/h) [11]. A Pd/TiO₂ NPs photocatalyst was synthesized by an ionic liquid assisted hydrothermal method, with promising H₂ evolution of 1250 μmol/g from the water-ethanol system under the illumination of visible light source [2]. The composites of rhodium-doped-TiO₂ nanostructures were fabricated by the sol-gel (nanoparticles) and hydrothermal (nanotubes) methods, with remarkable photocatalytic activity for H₂ generation from ethanol aqueous solutions [12]. The corresponding hydrogen evolution rates are 7246 μmol/g/h and 4856 μmol/g/h, respectively, which are 4 and 7 times higher than that of nanocrystals and nanotubes TiO₂.

In recent years, diverse Co species catalysts have been reported for photocatalytic H₂ production, which includes cobalt compounds and composites. For example, a cobaloxime complex-modified ruthenium dye-sensitized TiO₂ NPs catalyst was prepared by self-assembled method and exhibited excellent photocatalytic activity in pH neutral water and at room temperature under visible light irradiation [13]. The cobalt lactate complex/CdS nanorod photocatalyst showed high photocatalytic activity in H₂ evolution from the water splitting under visible light irradiation and the rate of H₂ production is 15.59 mmol/g/h, which is 3 times higher than the of

* Corresponding authors at: State Key Laboratory of Solid Waste Reuse for Building Materials, Beijing Building Materials Academy of Science Research, Beijing 100041, China (J. Guo).

E-mail addresses: guojianping@bmtbj.cn (J. Guo), boliu@bjtu.edu.cn (B. Liu).

that obtained with Pt/CdS photocatalyst [14]. A F-doping of Co_3O_4 films catalyst was prepared by chemical vapor deposition and displayed remarkable photocatalytic activity from ethanol in the near-ultraviolet region, which is 5 times hydrogen yield higher than undoped Co_3O_4 [15]. The noble-metal-free $\text{Co}(\text{OH})_2/\text{CdS}$ nanowires catalyst exhibited excellent hydrogen generation rate from water splitting under visible light irradiation, which is 206 times higher than the CdS NWs [16].

Hydrogen can be produced from diverse sources such as fossil fuels, oils, alcohols, water and biomass [17]. Organic compounds of methane and methanol as a substrate for H_2 generation by reforming reactions have been industrialized. However, as one of the most important bio-alcohols, ethanol is considered as a potential substrate for hydrogen evolution in terms of its renewability and lower toxicity. Various ethanol conversion technologies such as steam reforming, partial oxidation, autothermal reforming, alkaline-enhanced reforming, dehydrogenation, supercritical water gasification, photocatalysis and electrocatalysis have been widely used in H_2 production from ethanol [17]. Among the above mentioned technologies, because of its low cost and mild experimental conditions, the photocatalysis technology has great attractive for the ethanol conversion to H_2 generation. There are limited literatures available on exploring pure ethanol as raw material conversion to H_2 evolution. Through a facile photodeposition method, a new type Pt/ TiO_2 nanotube photocatalyst have been developed for photocatalytic hydrogen production from ethanol system by Lin and co-worker [18]. The research found that the preparation procedure of noble metal Pt loading catalyst has a significant effect on activity of hydrogen generation, the liquid phase product distribution and the catalyst stability. The nanosheet photocatalyst Pt/ TiO_2 was prepared by Xu etc., which demonstrated excellent catalytic activity for simultaneous H_2 production and selective oxidation of ethanol under the irradiation of sunlight [19].

Moreover, as one of the most important bio-alcohols, ethanol can be used to produce various chemicals through the oxidation process. Among them, the 1,1-diethoxyethane has attracted attention because of its special quality and extensive application. It could be used as raw material in organic synthesis and pharmaceutical industry [20]. From the environmental point of view, adding the 1,1-diethoxyethane to fuel can greatly reduce the emissions of particulate and nitrogen oxides. Generally, the two steps is needed for conversion of ethanol to 1,1-diethoxyethane. First the ethanol is oxidized to acetaldehyde, then the ethanol reacts with acetaldehyde to produce 1,1-diethoxyethane under the catalysis of acid. This indirect synthetic process is complexity and the oxidants are unfriendly to the environment. Therefore, the development of simple and green synthetic process is essential. Zhang's group has developed a new synthetic route. The noble-metal-loaded TiO_2 was synthesized by photodeposition method, with remarkable photocatalytic performance for the direct conversion of ethanol to 1,1-diethoxyethane under illumination of ultraviolet radiation [21].

In our previous reported work, the fibrous coordination polymer cobalt(II) diphenylphosphinate (denoted as CoDPPA) was prepared and the compound has excellent photocatalytic activity for H_2 production from ethanol solution, and ethyl acetate was produced in the same catalytic process [22]. For developing the catalytic performance of CoDPPA further, based on the band gap characteristics and optical properties of CoDPPA and TiO_2 , we designed and synthesized the CoDPPA/ TiO_2 composite. The three novel CoDPPA/ TiO_2 composites were prepared by the solvothermal and characterized through various methods. By the studies of hydrogen generation activity in ethanol solution, the composites exhibited the higher photocatalytic activity for H_2 production compared with CoDPPA or TiO_2 . Meanwhile, the side catalytic product 1,1-diethoxyethane was obtained. The possible photocatalytic

mechanism of the composite was proposed through the study of the optical properties.

2. Experimental

2.1. General procedures

All chemicals used were of reagent grade, purchased from Aladdin or Beijing Chemical Company. The actual chemical compositions were measured by Inductively Coupled Optical Emission Spectrometer (ICP-OES) on a PerkinElmer Optima 8000. The size and morphology of the composites were investigated using a Hitachi S-3400N microscope scanning electron microscope (SEM). Chemical state analysis and relative atomic ratio were carried out by X-ray photoelectron spectroscopy (XPS) in an AXIS Supra X-ray photoelectron spectrometer. The detailed spectra of C1s, O1s, P2p, Ti2p and Co2p were recorded in the following conditions. Based on a Shirley-type background [23], the raw spectra were fitted using nonlinear least-squares fitting program adopting Gaussian-Lorentzian peak shapes for all the peaks. Thermogravimetric analysis (TG) was performed on a TA Q500 apparatus between 20 and 800 °C with a heating rate of 10 K/min under N_2 atmosphere. The powder XRD patterns were obtained on a Rigaku Ultima IV X-ray diffractometer in transmission mode (flat sample holders, Cu-K α radiation) equipped with the D/tex Ultra detector (resolution 0.0001° in 2θ). The accelerating voltage and current were 40 kV and 40 mA, respectively. Infrared spectroscopy (IR) was measured on a Thermo Scientific Nicolet iS10 at the range of 400–4000 cm^{-1} . Elemental analysis (EA) was obtained by a Vario EL-III analysis apparatus. The UV-vis diffuse reflectance spectra (DRS) was performed on a PE Lambda 365 spectrophotometer, which was equipped with an integrating sphere and a standard white board was used as a reference. The photoluminescence (PL) spectra were measured by FLS980 Spectrometer with a xenon arc lamp (Xe900) and the entrance slit and the exit slit are both 4 nm.

2.2. Preparation of cobalt(II) diphenylphosphinate/ TiO_2

The composite of CoDPPA/ TiO_2 was prepared in following steps. Cobalt(II) chloride hexahydrate (0.0476 g, 0.2 mmol), diphenylphosphinic acid (denoted as DPPA) (0.0873 g, 0.4 mmol) were dissolved in 7 mL ethanol. Then a different amount of commercial P25 (TiO_2), with molar ratio of Co/Ti = 1/X (X = 1, 5, 10) was added to the solution, respectively. After ultrasonic and stirring, the mixture was transferred into a 15 mL Teflon lined stainless steel autoclave. The autoclave was sealed, maintained at 180 °C for 3 days, and cooled to room temperature naturally. The products were collected by filtration, washed with ethanol and dried in air. The prepared samples with the molar ratio Co/Ti of 1, 0.2 and 0.1 were labeled as CoTi1, CoTi5 and CoTi10, respectively. The EA results of the corresponding samples are as follows. Calcd. for CoTi1: C 50.29, H 3.52; found: C 44.65, H 3.11. Calcd. for CoTi5: C 32.19, H 2.26; found: C 16.08, H 1.13. Calcd. for CoTi10: C 22.31, H 1.56; found: C 8.09, H 0.60. The actual concentrations of Co and Ti in the composites were given by ICP-OES, the ratio of Co/Ti is basically the same as that of C and H to Ti.

2.3. Photocatalytic H_2 evolution

The photocatalytic hydrogen evolution test was carried out in a closed system of evacuation and gas circulation. A 300 W Xenon lamp was used as light source. In detail, 50 mg CoDPPA/ TiO_2 composite was dispersed in ethanol solution (100 mL). The suspension solution was sealed in a quartz vessel and purged with N_2 for 30 min to drive away the residual oxygen. The temperature of reac-

tion was kept at 20 °C by using cooling water. The gas product was analyzed periodically by a Shimadzu GC-14C (photocatalytic H₂ evolution amount in Fig. 9a and b) or GC-9790II (photocatalytic H₂ evolution recycling in Fig. 9c) gas chromatograph with the TCD detector.

3. Results and discussion

3.1. Synthesis and structure

The composites of CoDPPA/TiO₂ were synthesized by a simple solvothermal method. The nominal Co/Ti molar ratio of CoTi1, CoTi5 and CoTi10 are 1, 0.2 and 0.1, respectively. The actual concentrations of Co and Ti in the composites were given by ICP-OES, and the actual molar ratio of Co/Ti in CoTi1, CoTi5 and CoTi10 were 0.50, 0.09 and 0.03, respectively. These ratios were ascertained by the elemental analysis results of C and H in the composites. The proportion of cobalt in the composites is lower than the theoretical value, which is due to the synthesis of CoDPPA has a certain yield [22].

The XRD analyses of CoDPPA, TiO₂ and three composites were carried out and the graphs were combined together (Fig. 1). The CoDPPA has a strong peak at $2\theta = 8.02^\circ$, which is the characteristic peak of diphenylphosphonate metal salt [24]. In the XRD pattern of TiO₂, the diffraction peaks at 25.28°, 37.80°, 48.05°, 53.9°, 55.06°, 62.69° and 75.03° can be attributed to the (101), (004), (200), (105), (211), (204) and (215) crystal planes of anatase TiO₂ (JCPDS No. 21-1272) [25], respectively. The peak positions of the three composites correspond to the sum of XRD peak of CoDPPA and TiO₂, indicating the solvothermal process didn't affect the crystal structure of CoDPPA and TiO₂ [26]. Moreover, the characteristic peak intensity of CoDPPA decreases with the increase of Ti/Co molar ratio.

The infrared spectra of CoDPPA, TiO₂ and CoTi10 were shown in Fig. 2. In the spectrum of CoDPPA, the peaks at 3053 cm⁻¹ and 1593 cm⁻¹ can be attributed to the characteristic C–H and C=C bonds on benzene ring. The peak at 1437 cm⁻¹ can be attributed to the characteristic vibration of benzene ring skeleton. The strong peak at 1053 cm⁻¹ is the characteristic absorption peak of Co–O–P bridge structure. The absorption peaks at 1625 cm⁻¹ and 500–700 cm⁻¹ are the characteristic peaks of TiO₂. The peak at 1625 cm⁻¹ can be attributed to O–H stretching vibration, which is produced by the presence of water adsorbed on the surface of

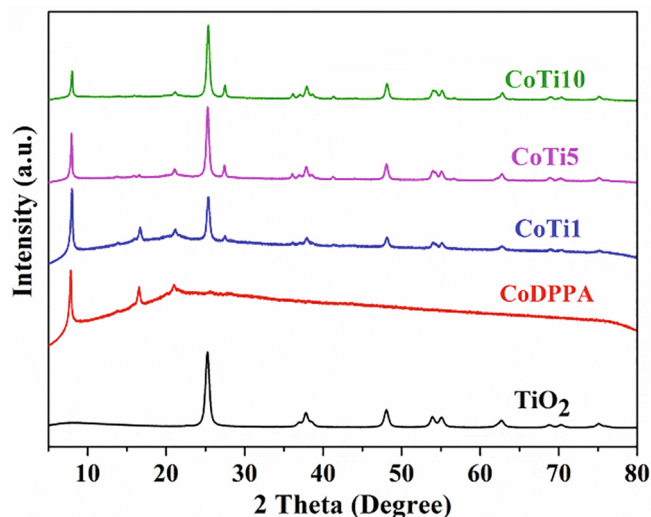


Fig. 1. XRD patterns of CoDPPA, TiO₂, CoTi1, CoTi5 and CoTi10.

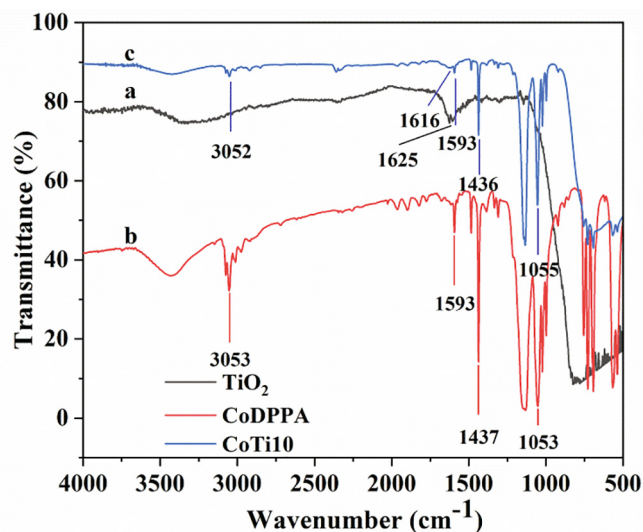


Fig. 2. IR spectra of (a) TiO₂, (b) CoDPPA and (c) CoTi10.

titanium dioxide. The absorption peaks contains in the composite CoTi10 spectrum correspond to the sum of the CoDPPA and TiO₂. The peaks at 3052 cm⁻¹ and 1593 cm⁻¹ can be attributed to the characteristic C–H and C=C bonds on benzene ring. The absorption peak at 1616 cm⁻¹ can be attributed to O–H stretching vibration of water adsorbed on the surface of CoTi10. The peak at 1436 cm⁻¹ can be attributed to the characteristic vibration of benzene ring skeleton. The peak at 1055 cm⁻¹ is the characteristic absorption peak of Co–O–P bridge structure.

To further understand the bonding form of composites, XPS testing was implemented. The XPS patterns of CoTi10 were shown in Fig. 3. The data of CoTi10 show that this composite contain C, O, P, Co and Ti elements. In the high-resolution spectrum of Ti (Fig. 3e), two peaks of binding energy 458.8 eV and 464.7 eV are allocated to Ti2p3/2 and Ti2p1/2. The spin energy separation of 5.9 eV between Ti2p3/2 and Ti2p1/2 suggests that Ti ions adopt the 4+ oxidation state in the composite [27–30]. In the high-resolution spectrum of Co (Fig. 3f), the fitting peaks of Co2p3/2 and Co2p1/2 are at 780.9 eV and 796.3 eV, respectively. Compared with the high-resolution spectrum of CoDPPA, the fitting peaks position of Co are shifted, which may be caused by the interaction between CoDPPA and TiO₂. The spin orbit separation energy between the two peaks is 15.4 eV, indicating that Co element on the composite surface exists as Co²⁺ [31–34].

3.2. Morphology analysis

The morphologies of CoDPPA and three composites were investigated by SEM and the images were presented in Fig. 4. The surface of the fibrous CoDPPA is smooth and the diameter ranges varies from hundreds of nanometers to several microns. From the images of the composites, it can be observed that the surface of the fibrous CoDPPA was coated with irregular TiO₂ granular. The surfaces of the composites are coarser with respect to the CoDPPA.

In order to further understand the combination of CoDPPA and TiO₂, EDS area scanning were carried out and the images of the composite CoTi10 were shown in Fig. 5. Five elements of C, O, P, Co and Ti appeared in the scanning pictures. The distribution shape of five elements is basically uniform and similar to the SEM shape of the composite, which indicated that the composition of CoDPPA and TiO₂ composite is uniform.

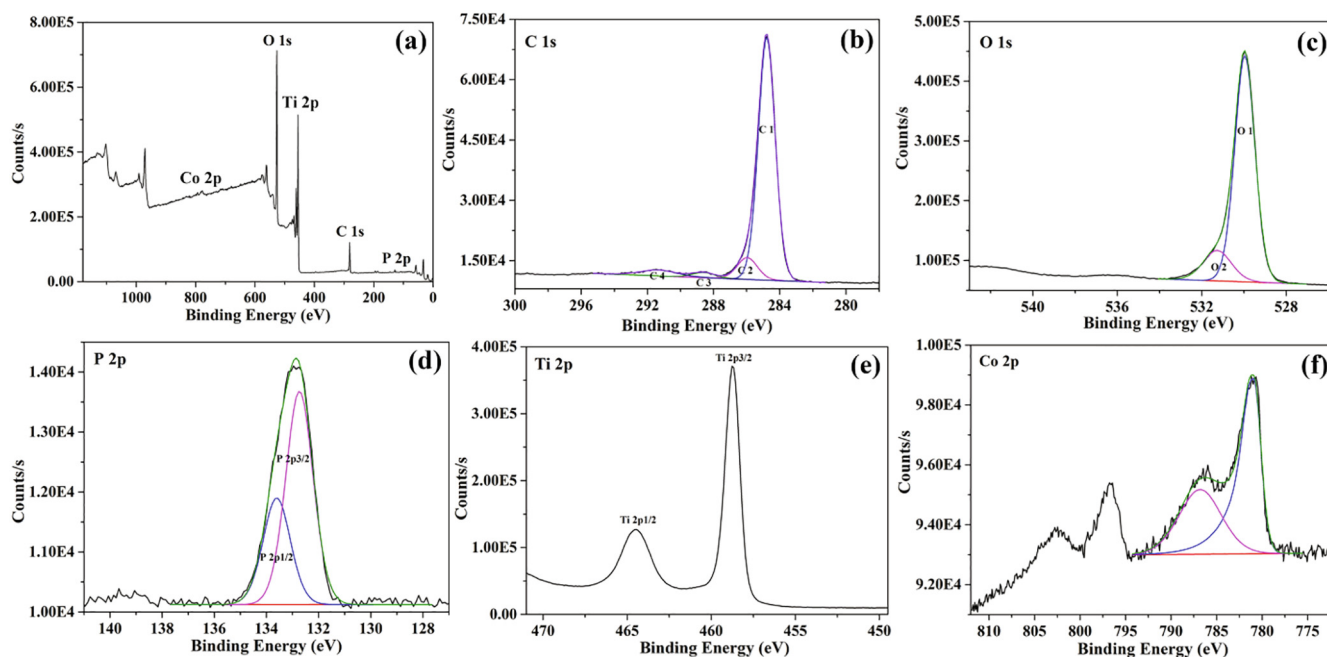


Fig. 3. XPS patterns of CoTi10 (a) wide of the XPS, (b) C1s, (c) O1s, (d) P2p, (e) Ti2p and (f) Co2p.

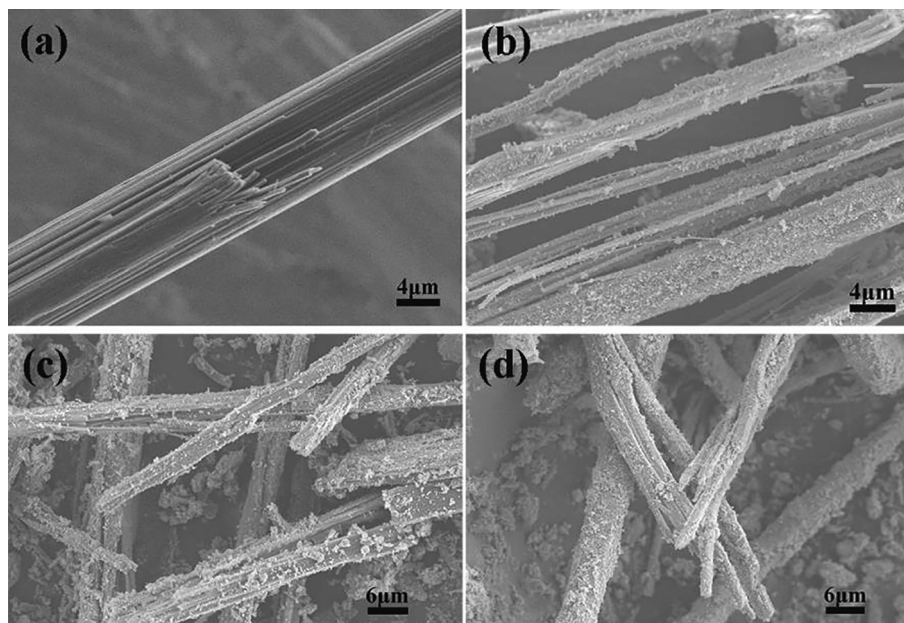


Fig. 4. SEM images of (a) CoDPPA, (b) CoTi1, (c) CoTi5 and (d) CoTi10.

3.3. Thermal behavior of CoDPPA/TiO₂

The thermal stability of CoDPPA and three composites were studied by thermo gravimetric analysis (Fig. 6). Although the molar ratio of each product is different, the trends of TG curves are basically consistent. It can be observed that the decomposition of CoDPPA and composites is one-step reaction in N₂, which can be ascribed to the thermal decomposition of organic component in the material. The T_{max} of CoDPPA is 604 °C, the total weight loss is 76.80% and the residue is 23.20%. With the increase of Ti/Co molar ratio, the residue of composite increases correspondingly. The total weight loss of CoTi1, CoTi5 and CoTi10 are 48.50%, 15.55% and 4.44%, respectively, and the corresponding residues

are 51.50%, 84.45% and 95.56%. The T_{max} of CoTi1, CoTi5 and CoTi10 are 602 °C, 632 °C and 664 °C, respectively. This indicates the composites have good thermal stability under N₂ in terms of its decomposition temperature.

3.4. Optical properties of CoDPPA/TiO₂

The optical properties of CoDPPA, TiO₂ and three composites were studied by UV–vis diffuse reflectance spectra (DRS). As shown in Fig. 7a, it is obvious that TiO₂ could only absorb UV light up to 408 nm, which mainly belonged to the UV region due to its wide energy band gap (3.12 eV) [35] and was unlikely to respond to visible light. The absorption edge of three composites could reach

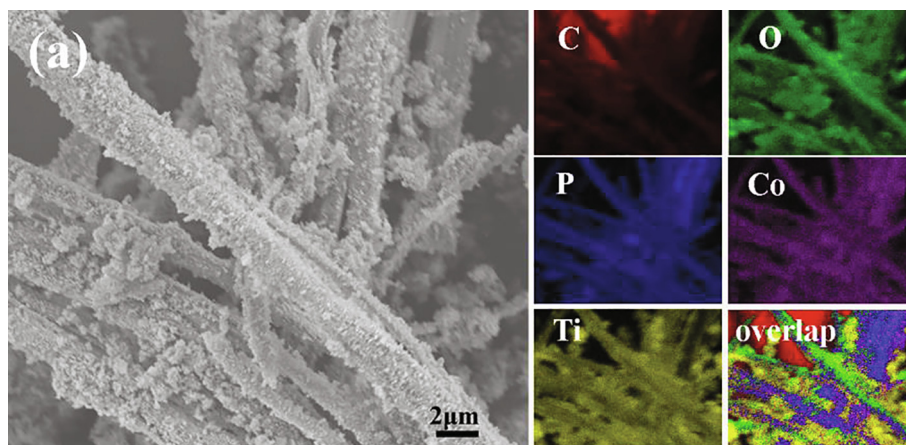


Fig. 5. EDX mapping images of CoTi10.

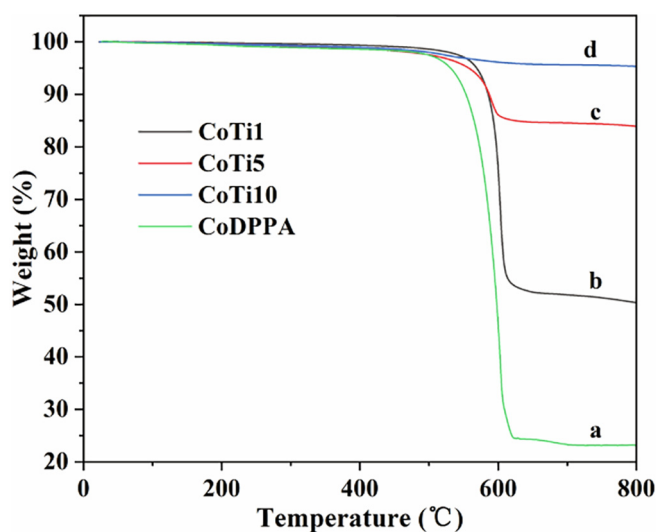


Fig. 6. TG curves of (a) CoDPPA, (b) CoTi1, (c) CoTi5 and (d) CoTi10.

410 nm (CoTi1), 417 nm (CoTi5) and 422 nm (CoTi10), respectively, arising from the band absorption [36]. The absorption edges move to longer wavelengths than that of TiO_2 implies the decrease of the band gap due to the combination with CoDPPA. The indirect band gap values could be obtained by the Tauc equation ($\alpha h\nu = A (h\nu - E_g)^2$) using the UV–Vis absorption data [37].

By making the tangent of the $(\alpha h\nu)^{1/2}$ versus $h\nu$ curves and extending to X-axis, the indirect band gap values could be determined. The band gap of CoDPPA, TiO_2 , CoTi1, CoTi5 and CoTi10 as a key factor of photocatalytic activity were measured 1.80, 3.12, 3.20, 3.02 and 2.92 eV, respectively (Fig. 7b) [38]. The resulting data showed the band gap of CoTi5 and CoTi10 photocatalyst are lower than pure TiO_2 , which implied the red shift of absorption in the visible light region [39]. That is the CoTi5 and CoTi10 composites could effectively absorb and utilize incident light, to generate more photo electrons and holes, and exhibit the better photocatalytic properties than TiO_2 .

The PL measurement of the photocatalysts could indicate the existence of surface defects, oxygen vacancies, migration and the recombination processes of the photogenerated electrons and holes on the samples [40,41]. The PL spectra of CoDPPA, TiO_2 and three composites were shown in Fig. 8 with the excitation wavelength of 350 nm. In general, the emission intensity of PL is inversely correlated with the photocatalytic activity [42,43], and the lower PL intensity corresponds to higher separation efficiency [44], which is favorable for photocatalytic activity. It was observed that the composites exhibited much lower emission intensity than that of TiO_2 (Fig. 8).

In comparison with the optical properties of pure TiO_2 , the composites can effectively suppress the recombination of photogenerated electrons and holes and thus improve the photocatalytic activity. The results are consistent with the photocatalytic hydrogen production of the composites.

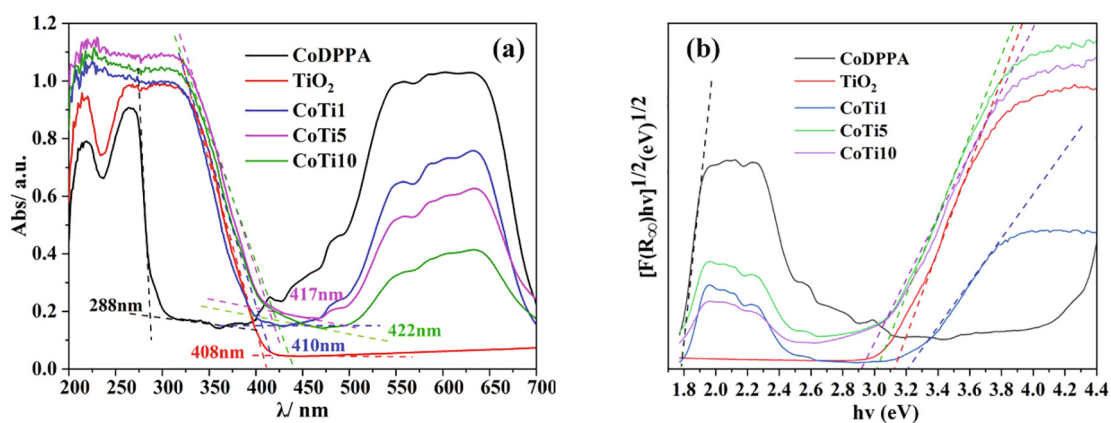


Fig. 7. (a) UV–vis DRS spectra of CoDPPA, TiO_2 , CoTi1, CoTi5 and CoTi10, (b) band gap spectra of CoDPPA, TiO_2 , CoTi1, CoTi5 and CoTi10.

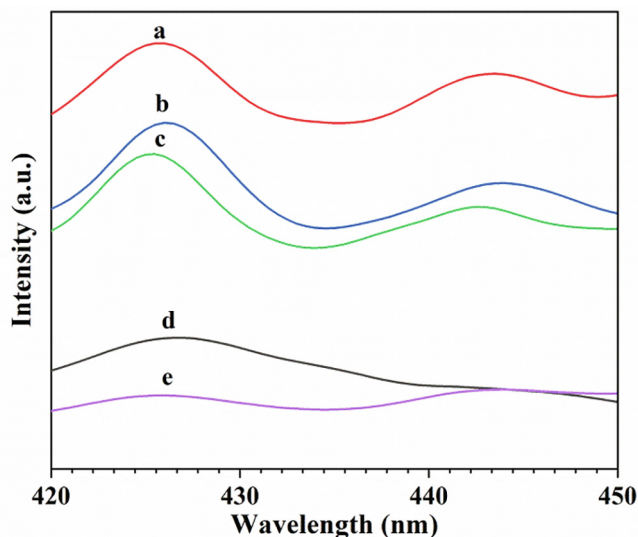


Fig. 8. PL spectroscopy of (a) TiO_2 , (b) CoTi1, (c) CoTi5, (d) CoDPPA and (e) CoTi10.

3.5. Photocatalytic property of CoDPPA/ TiO_2

The photocatalytic H_2 generation activities of CoDPPA, TiO_2 and three composites have been tested under UV–visible light irradiation. As shown in Fig. 9a, under irradiation for 3 h, the quantity of photocatalytic H_2 evolution by TiO_2 and CoDPPA is $92.26 \mu\text{mol/g}$ and $165.30 \mu\text{mol/g}$, respectively. However, the composites with the higher Ti/Co molar ratio showed better photocatalytic activity in H_2 evolution under the same conditions, the quantity of H_2 production by CoTi5 and CoTi10 is $515.94 \mu\text{mol/g}$ and $1155.86 \mu\text{mol/g}$, respectively.

Gas chromatogram and Mass spectrogram of liquid products of photocatalyzed ethanol by CoTi10 were shown in Fig. 10. It shows that the liquid product has a strong peak at retention time of 4.203 min (Fig. 10a). This product was confirmed to be 1,1-diethoxyethane (denoted as DEE) by GC–MS analysis (Fig. 10b). Moreover, the quantitative analysis of GC–MS showed that the concentration of DEE was 2950.05 mg/L and the conversion rate of ethanol is 0.39% after 780 min UV–Vis irradiation.

The stabilities of the composite CoTi10 were evaluated through long-term and recycling test of photocatalytic H_2 generation. In the long-term hydrogen production test, the hydrogen production of composite CoTi10 did not decrease after 12 h (Fig. 9b). In the cycle test, the experimental result showed that the composite maintained relative stable H_2 generation abilities after 3 cycles with 12 h as a cycle, and its hydrogen production remains at 94% (Fig. 9c). For CoTi10, the hydrogen production is $5472.14 \mu\text{mol/g}$

under UV–visible light irradiation for 12 h. This demonstrated that the composite CoTi10 not only has better photocatalytic performance than the TiO_2 , but also can maintain the long time and multiple cycle stability.

Moreover, the stability of the composite was also estimated using IR. With CoTi10 as the representative, the IR spectra of the composite before and after the photocatalytic H_2 evolution under UV–visible light irradiation were shown in Fig. 11. It was observed that the CoTi10 exhibits substantially unchanged before and after the photocatalytic H_2 production, suggesting the good stability of the composite. There are no new peaks in the IR spectrum of after photocatalytic hydrogen generation, indicating that no new functional groups are formed.

In order to compare the difference of photocatalytic properties of the composite and mechanical mixture of CoDPPA and TiO_2 , the CoDPPA and TiO_2 mixture sample with molar ratio of 1:10 were evenly grinded in agate mortar and the photocatalytic experiment was carried out under the same conditions. Under UV–visible light irradiation for 3 h, the quantity of photocatalytic H_2 generation catalyzed by the mixture is $817.66 \mu\text{mol/g}$. It is lower than that of the composite CoTi10 ($1155.86 \mu\text{mol/g}$). Furthermore, the stability test showed that the hydrogen evolution of the mixture began to decrease after 12 h of illumination, but that of the composite CoTi10 was increasing. It is evidently that the photocatalytic H_2 production properties of the mixture are difference from the composite CoTi10.

3.6. Photocatalytic mechanism of CoDPPA/ TiO_2

Generally, two typical components are involved in the photocatalysis process. The energy band gap should be suitable for the electrons and holes production under irradiation. And the energy level should be satisfied for the redox of protons. The value of the highest occupied molecular orbital (HOMO) and lowest unoccupied molecular orbital (LUMO) energy level of the composites are relevant for photocatalytic hydrogen production. The UV–vis spectra of the composites are recorded with well-defined optical adsorption associated with the LUMO–HOMO gap and the band gap was assessed based on the relation $E_g = 1240/\lambda$ [45–47].

A potential photocatalytic mechanism was suggested as shown in Fig. 12. The electrons are excited from the valence band to the conduction band of TiO_2 under UV–visible light irradiation. Since the redox potential of $\text{Co}^{2+}/\text{Co}^+$ (-0.43 V vs SHE) [48,49] is lower than that of the conduction band level of TiO_2 (about -0.6 V), the photons induced electrons in the conduction band of TiO_2 can be efficiently transferred to CoDPPA. The ligand-to-metal charge transfer route with similar components has been proposed by Huang's group [44]. The photogenerated electrons from TiO_2 transfer to benzene ring of ligand and then to cobalt(II) and make the formation of cobalt(I). This will lead to the circular photocat-

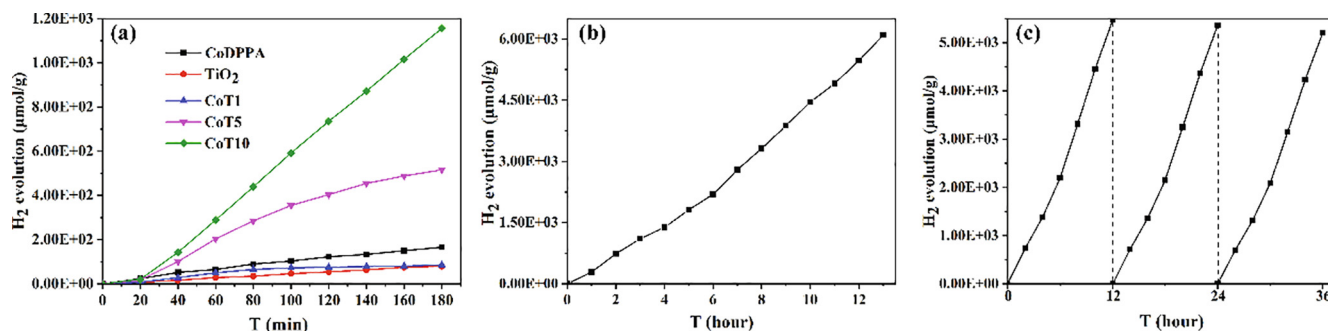


Fig. 9. (a) Plots of photocatalytic H_2 evolution amount versus UV–visible light irradiation time by various samples, (b) Plots of photocatalytic H_2 evolution amount from CoTi10 for 13 h under UV–visible light irradiation and (c) Recycling photocatalytic H_2 evolution reactions of CoTi10 under UV–visible light irradiation.

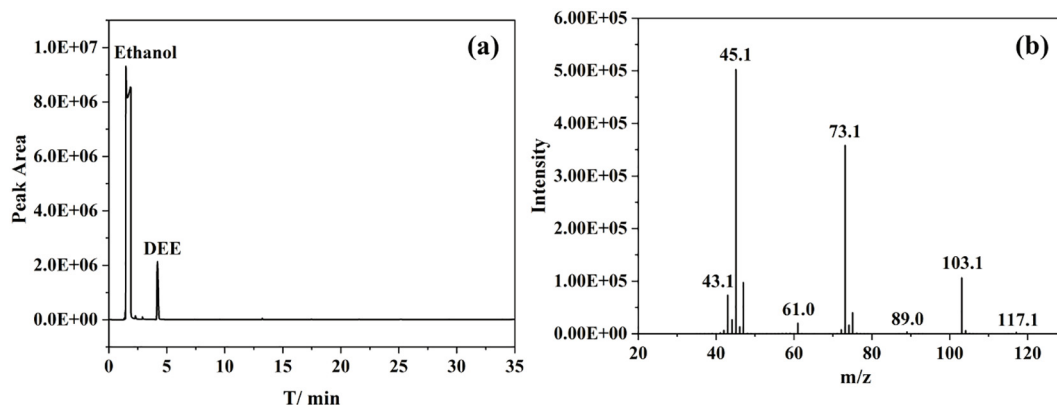


Fig. 10. Gas chromatogram and Mass spectrogram of liquid products catalyzed by CoTi10.

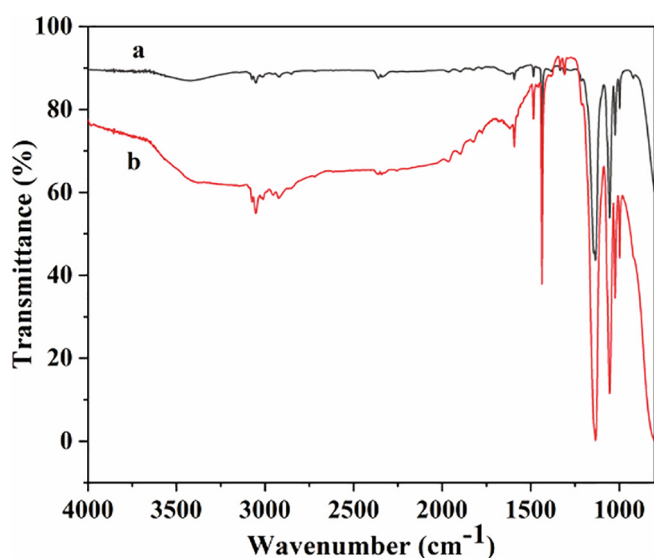


Fig. 11. IR spectra of CoTi10 (a) before and (b) after photocatalytic H₂ production under UV-visible light irradiation.

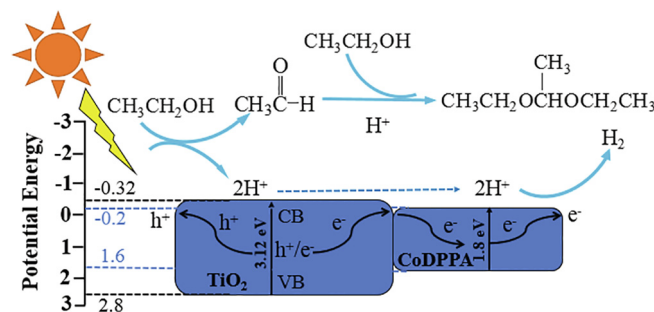


Fig. 12. Schematic illustration of photocatalytic H₂ generation and DEE by CoDPPA/TiO₂ under UV-visible light irradiation.

alytic reactions of Co²⁺ and Co⁺ [50–52]. Multivalent cobalt compounds can accelerate the separation and transference of photo-generated electrons at the interface between TiO₂ and cobalt compounds, leading to improve the photocatalytic activity. Meanwhile, the holes in the valence band of TiO₂ have strong oxidation, which can directly oxidize ethanol to acetaldehyde and H⁺. Under the catalysis of H⁺ produced in situ, acetaldehyde with unreacted ethanol to form 1,1-diethoxyethane. It can be inferred that as the

co-catalyst, the CoDPPA provides active sites for H₂ generation and causes the transference of photogenerated electrons from TiO₂ toward CoDPPA, which can be effectively inhibit the recombination of photogenerated electrons and holes and lead to the enhancement of photocatalytic activity [53–58].

4. Conclusions

According to the band gap characteristics and photocatalytic properties of CoDPPA and TiO₂, Co (II) diphenylphosphonate/TiO₂ composites were designed and prepared by solvothermal method. The study of optical properties of the composites showed that the composites can effectively suppress the recombination of photo-generated electrons and holes and enhance the photocatalytic activity. The experimental results indicated that the composites have remarkable photocatalytic H₂ production activity relative to the compound CoDPPA or TiO₂. Furthermore, the by-product 1,1-diethoxyethane was produced with unique selectivity in the photocatalytic process. This work demonstrated that the composites as photocatalyst have the important application in the photocatalytic conversion of ethanol.

Declaration of Competing Interest

The authors declare that they have no known competing financial interests or personal relationships that could have appeared to influence the work reported in this paper.

Acknowledgments

This work was funded by Natural Science Foundation of China (20872084 to J.-P. Guo) and Beijing Building Materials Academy of Science Research. The XPS determination and analysis were supported by Shimadzu.

References

- [1] X. Zhang, Y. Sun, X. Cui, Z. Jiang, A green and facile synthesis of TiO₂/graphene nanocomposites and their photocatalytic activity for hydrogen evolution, *Int. J. Hydrogen Energy* 37 (1) (2012) 811–815.
- [2] T.N. Ravishankar, M.D.O. Vaz, T. Ramakrishnappa, S.R. Teixeira, J. Dupont, G. Banuprakash, The heterojunction effect of Pd on TiO₂, for visible light photocatalytic hydrogen generation via water splitting reaction and photodecolorization of trypan blue dye, *J. Mater. Sci. Mater. Elem.* 29 (13) (2018) 11132–11143.
- [3] W.T. Chen, A. Chan, D.X. Sun-Waterhouse, J. Llorca, H. Idriss, G.I.N. Waterhouse, Performance comparison of Ni/TiO₂ and Au/TiO₂ photocatalysts for H₂ production in different alcohol-water mixtures, *J. Catal.* 367 (2018) 27–42.
- [4] A. Fujishima, K. Honda, Electrochemical photolysis of water at a semiconductor electrode, *Nature* 238 (5358) (1972) 37–38.

- [5] N. Stratakis, V. Bekiaris, D.I. Kondarides, P. Lianos, Hydrogen production by photocatalytic alcohol reforming employing highly efficient nanocrystalline titania films, *Appl. Catal. B* 77 (1–2) (2007) 184–189.
- [6] L. Martínez, L. Soler, I. Angurell, J. Lester, Effect of TiO₂ nanoshape on the photoproduction of hydrogen from water-ethanol mixtures over Au₃Cu/TiO₂ prepared with preformed Au-Cu alloy nanoparticles, *Appl. Catal. B: Environ.* 248 (2019) 504–514.
- [7] Y. Ma, X. Wang, Y. Jia, X. Chen, H. Han, C. Li, Titanium dioxide-based nanomaterials for photocatalytic fuel generations, *Chem. Rev.* 114 (19) (2014) 9987–10043.
- [8] V. Raj, T. Lu, M. Lockrey, R. Liu, F. Kremer, L. Li, Y. Liu, H. Tan, C. Jagadish, Introduction of TiO₂ in CuI for its improved performance as a p-type transparent conductor, *ACS Appl. Mater. Interfaces* 11 (27) (2019) 24254–24263.
- [9] J.M. Kim, J.K. Hwang, Y.K. Yang-Kook Sun, J. Hassoun, A single layer of Fe₃O₄@TiO₂ submicron spheres as a high-performance electrode for lithium-ion microbatteries, *Sustain. Energy Fuels* 3 (2019) 2675–2687.
- [10] W.Z. Geng, H.C. Jiang, X. Yang, Y. Feng, X.Y. Wang, Z. Geng, Self-cleaning antifouling TiO₂/poly(aryl ether sulfone) composite ultrafiltration membranes, *Chem. Res. Chin. Univ.* 35 (4) (2019) 714–720.
- [11] S.H. Chen, Y. Xiao, Y.H. Wang, W. Zhang, Z.F. Hu, H. Zhao, W. Xie, Ethanol-quinching modified the surface environment of titanium dioxide for visible light-assisted hydrogen production, *Catal. Sci. Technol.* 9 (16) (2019) 4222–4225.
- [12] R. Camposeco, S. Castillo, V. Rodriguez-Gonzalez, M. Hinojosa-Reyes, I. Mejía-Centeno, Tailored TiO₂ nanostructures for supporting Rh₃O₂ and Rh⁰ nanoparticles: enhanced photocatalytic H₂ production, *J. Photochem. Photobiol. A* 356 (2018) 92–101.
- [13] F. Lakdamyali, E. Reisner, Photocatalytic H₂ evolution from neutral water with a molecular cobalt catalyst on a dye-sensitised TiO₂ nanoparticle, *Chem. Commun.* 47 (6) (2011) 1695–1697.
- [14] L. Wang, N. Xu, X.Y. Pan, Y.S. He, X.X. Wang, W.Y. Su, Cobalt lactate complex as hole cocatalyst for significantly enhanced photocatalytic H₂-production activity over CdS nanorods, *Catal. Sci. Technol.* 8 (6) (2018) 1599–1605.
- [15] A. Gasparotto, D. Barreca, D. Bekermann, A. Devi, R.A. Fischer, P. Fornasiero, V. Gombac, O.I. Lebedev, C. Maccato, T. Montini, G.V. Tendeloo, E. Tondello, F-doped Co₃O₄ photocatalysts for sustainable H₂ generation from water/ethanol, *J. Am. Chem. Soc.* 133 (48) (2011) 19362–19365.
- [16] X. Zhou, J. Jin, X.J. Zhu, J. Huang, J.G. Yu, W.Y. Wong, W.K. Wong, New Co(OH)₂/CdS nanowires for efficient visible light photocatalytic hydrogen production, *J. Mater. Chem. A* 4 (14) (2016) 5282–5287.
- [17] S. Nanda, R. Rana, Y. Zheng, J.A. Kozinski, A.K. Dalai, Insights on the pathways for hydrogen generation from ethanol, *Sustain. Energy Fuels* 1 (6) (2017) 1232–1245.
- [18] C.H. Lin, C.H. Lee, J.H. Chao, C.Y. Kuo, Y.C. Cheng, W.N. Huang, H.W. Chang, Y.M. Huang, M.K. Shi, Photocatalytic generation of H₂ gas from neat ethanol over Pt/TiO₂ nanotube catalysts, *Catal. Lett.* 98 (1) (2004) 61–66.
- [19] Xu Y. J., Weng B. X., Photocatalysts for simultaneous hydrogen production and selective oxidation of ethanol and their preparation methods, CN 106111129 A [p], 2016-6-28.
- [20] (a) F. Frusteri, L. Spadaro, C. Beatrice, C. Guido, Oxygenated additives production for diesel engine emission improvement, *Chem. Eng. J.* 134 (1–3) (2007) 239–245; (b) V.M.T.M. Silva, A.E. Rodrigues, Synthesis of diethylacetal: thermodynamic and kinetic studies, *Chem. Eng. Sci.* 56 (4) (2001) 1255–1263.
- [21] H.X. Zhang, Y.P. Wu, L. Li, Z.P. Zhu, Photocatalytic direct conversion of ethanol to 1,1-diethoxyethane over noble-metal-loaded TiO₂ nanotubes and nanorods, *ChemSusChem* 8 (7) (2015) 1226–1231.
- [22] A.H. Li, D.Y. Li, J.P. Han, R.D. Xue, B. Liu, J.P. Guo, Solvothermal synthesis, structural characterization and photocatalysis of fibrous cobalt(II) diphenylphosphinate, *Polyhedron* 178 (2020) 114339–114346.
- [23] D.A. Shirley, High-resolution X-ray photoemission spectrum of the valence bands of gold, *Phys. Rev. B* 5 (12) (1972) 4709–4714.
- [24] Y. Zhang, C.Q. Zhao, Y.W. Huang, Preparation and characterization of metal phosphonate nano-hybrid materials with controlled morphology, *Fine Chem.* 33 (2016) 1–7.
- [25] L. Ling, Y. Wang, W. Zhang, Z.M. Ge, W.B. Duan, B. Liu, Preparation of a novel ternary composite of TiO₂/UiO-66-NH₂/graphene oxide with enhanced photocatalytic activities, *Catal. Lett.* 148 (7) (2018) 1978–1984.
- [26] X.B. Chen, L. Liu, P.Y. Yu, S.S. Mao, Increasing solar absorption for photocatalysis with black hydrogenated titanium dioxide nanocrystals, *Science* 331 (6018) (2011) 746–750.
- [27] H. Li, Z. Chen, C.K. Tsang, Z. Li, X. Ran, C. Lee, B. Nie, L.X. Zheng, T. Hung, J. Lu, B. C. Pan, Y.Y. Li, Electrochemical doping of anatase TiO₂ in organic electrolytes for high-performance supercapacitors and photocatalysts, *J. Mater. Chem. A* 2 (1) (2014) 229–236.
- [28] H.Y. He, J.H. Lin, W. Fu, X.L. Wang, H. Wang, Q.S. Zeng, Q. Gu, Y.M. Li, C. Yan, B. K. Tay, C. Xue, X. Hu, S.T. Pantelides, W. Zhou, Z. Liu, MoS₂/TiO₂ edge-on heterostructure for efficient photocatalytic hydrogen evolution, *Adv. Energy Mater.* 6 (14) (2016) 1600464–1600471.
- [29] F.B. Li, X.Z. Li, M.F. Hou, Photocatalytic degradation of 2-mercaptobenzothiazole in aqueous La³⁺-TiO₂ suspension for odor control, *Appl. Catal. B: Environ.* 48 (3) (2004) 185–194.
- [30] G.S. Li, D.Q. Zhang, J.C. Yu, A new visible-light photocatalyst: CdS quantum dots embedded mesoporous TiO₂, *Environ. Sci. Technol.* 43 (18) (2009) 7079–7085.
- [31] C.D. Wagner, W.M. Riggs, L.E. Davis, J.F. Moulder, G.E. Muilenberg, Handbook of X-Ray Photoelectron Spectroscopy, Perkin-Elmer Corporation Physical Electronics Division, U.S.A., 1979, p. 78.
- [32] D. Barreca, C. Massignan, S. Daolio, M. Fabrizio, C. Piccirillo, L. Armelao, E. Tondello, Composition and microstructure of cobalt oxide thin films obtained from a novel cobalt(II) precursor by chemical vapor deposition, *Chem. Mater.* 13 (2) (2001) 588–593.
- [33] K.S. Kim, X-ray-photoelectron spectroscopic studies of the electronic structure of CoO, *Phys. Rev. B* 11 (6) (1975) 2177–2185.
- [34] A. Gulino, G. Fiorito, I. Fragalà, Deposition of thin films of cobalt oxides by MOCVD, *J. Mater. Chem.* 13 (4) (2003) 861–865.
- [35] G. Li, L. Wu, F. Li, P. Xu, D. Zhang, H. Li, Photoelectrocatalytic degradation of organic pollutants via a CdS quantum dots enhanced TiO₂ nanotube array electrode under visible light irradiation, *Nanoscale* 5 (5) (2013) 2118–2125.
- [36] J. Fang, L. Xu, Z. Zhang, Y. Yuan, S. Cao, Z. Wang, L. Yin, Y. Liao, C. Xue, Au@TiO₂-CdS ternary nanostructures for efficient visible-light-driven hydrogen generation, *ACS Appl. Mater. Interfaces* 5 (16) (2013) 8088–8092.
- [37] J. Tauc, R. Grigorovici, A. Vancu, Optical properties and electronic structure of amorphous germanium, *Phys. Status Solidi B* 15 (2) (1966) 627–637.
- [38] M. Shang, W. Wang, L. Zhou, S. Sun, W. Yin, Nanosized BiVO₄ with high visible-light-induced photocatalytic activity: ultrasonic-assisted synthesis and protective effect of surfactant, *J. Hazard. Mater.* 172 (1) (2009) 338–344.
- [39] P. Askari, S. Mohebbi, Porphyrin cobalt(II) complex linked to TiO₂/BiVO₄ nanocomposite: alcohol oxidation using nano-hybrid materials as implement photocatalyst with mechanism approach, *New J. Chem.* 42 (3) (2018) 1715–1724.
- [40] M. Long, W. Cai, J. Cai, B. Zhou, X. Chai, Y. Wu, Efficient photocatalytic degradation of phenol over Co₃O₄/BiVO₄ composite under visible light irradiation, *J. Phys. Chem. B* 110 (41) (2006) 20211–20216.
- [41] F. Duan, Y. Zheng, M. Chen, Flowerlike PtCl₄/Bi₂WO₆ composite photocatalyst with enhanced visible-light-induced photocatalytic activity, *Appl. Surf. Sci.* 257 (6) (2011) 1972–1978.
- [42] Q.C. Xu, D.V. Wellia, Y.H. Ng, R. Amal, T.T.Y. Tan, Synthesis of porous and visible-light absorbing Bi₂WO₆/TiO₂ heterojunction films with improved photoelectrochemical and photocatalytic performances, *J. Phys. Chem. C* 115 (15) (2011) 7419–7428.
- [43] R. Georgekuttty, M.K. Seery, S.C. Pillai, A Highly efficient Ag-ZnO photocatalyst: synthesis, properties, and mechanism, *J. Phys. Chem. C* 112 (35) (2008) 13563–13570.
- [44] J.J. Wang, R.Q. Zhang, Y.Y. Liu, Z.Y. Wang, P. Wang, Z.K. Zheng, X.Y. Qin, X.Y. Zhang, Y. Dai, B.B. Huang, Two transition metal phosphonate photocatalysts for H₂ evolution and CO₂ reduction, *Chem. Commun.* 54 (52) (2018) 7195–7198.
- [45] Q. Yu, H. Dong, X. Zhang, Y.X. Zhu, J.H. Wang, F.M. Zhang, X.J. Sun, Novel Stable metal-organic framework photocatalyst for light-driven hydrogen production, *CrystEngComm* 20 (23) (2018) 3228–3233.
- [46] M.L.K. Sanchez, C. Wu, M.W.W. Adams, R.B. Dyer, Optimizing electron transfer from CdSe QDs to hydrogenase for photocatalytic H₂ production, *Chem. Commun.* 55 (39) (2019) 5579–5582.
- [47] M.A. Nasalevich, M. Veen, F. Kapteijn, J. Gascon, Metal-organic frameworks as heterogeneous photocatalysts: advantages and challenges, *CrystEngComm* 16 (23) (2014) 4919–4926.
- [48] Z.J. Li, X.B. Li, J.J. Wang, S. Yu, C.B. Li, C.H. Tung, L.Z. Wu, A robust “artificial catalyst” in situ formed from CdTe QDs and inorganic cobalt salts for photocatalytic hydrogen evolution, *Energy Environ. Sci.* 6 (2) (2013) 465–469.
- [49] J.L. Dempsey, B.S. Brunschwig, J.R. Winkler, H.B. Gray, Hydrogen evolution catalyzed by cobaloximes, *Acc. Chem. Res.* 42 (12) (2009) 1995–2004.
- [50] J.R. Ran, J.G. Yu, M. Jaroniec, Ni(OH)₂ modified CdS nanorods for highly efficient visible-light-driven photocatalytic H₂ generation, *Green Chem.* 13 (10) (2011) 2708–2713.
- [51] H. Wender, R.V. Goncalves, C.S.B. Dias, M.J.M. Zapata, L.F. Zagonel, E.C. Mendonca, S.R. Teixeira, F. Garcia, Photocatalytic hydrogen production of Co(OH)₂ nanoparticle-coated α-Fe₂O₃ nanorings, *Nanoscale* 5 (19) (2013) 9310–9316.
- [52] J. Barrett, Inorganic chemistry in aqueous solution, periodicity of aqueous chemistry II: d-block chemistry, *R. Soc. Chem.* (2003) 136–138.
- [53] J. Wang, B. Li, J. Chen, N. Li, J. Zheng, J. Zhao, Z. Zhu, Enhanced photocatalytic H₂-production activity of Cd_{0.9}Zn_{0.1-x}S nanocrystals by surface loading MS (M = Ni, Cu) species, *Appl. Surf. Sci.* 259 (2012) 118–123.
- [54] M. Tabata, K. Maeda, T. Ishihara, T. Minegishi, T. Takata, K. Domen, Photocatalytic hydrogen evolution from water using copper gallium sulfide under visible-light irradiation, *J. Phys. Chem. C* 114 (25) (2010) 11215–11220.
- [55] S. Xu, D.D. Sun, Significant improvement of photocatalytic hydrogen generation rate over TiO₂ with deposited CuO, *Int. J. Hydrogen Energy* 34 (15) (2009) 6096–6104.
- [56] T. Morikawa, Y. Irokawa, T. Ohwaki, Enhanced photocatalytic activity of TiO_{2-x}N_x loaded with copper ions under visible light irradiation, *Appl. Catal. A: Gen.* 314 (1) (2006) 123–127.
- [57] J. Bandara, C.P.K. Udawatta, C.S.K. Rajapakse, Highly stable CuO incorporated TiO₂ catalyst for photocatalytic hydrogen production from H₂O, *Photochem. Photobiol. Sci.* 4 (11) (2005) 857–861.
- [58] J.G. Yu, J.G. Ran, Facile preparation and enhanced photocatalytic H₂-production activity of Cu(OH)₂ cluster modified TiO₂, *Energy Environ. Sci.* 4 (4) (2011) 1364–1371.